Head & Face Medicine

RESEARCH

Open Access

A novel 3D multimodal fusion imaging surgical guidance in microvascular decompression for primary trigeminal neuralgia and hemifacial spasm

Xiaolin Hou[1], Ru xiang Xu[1], Jing Tang[2] and Cheng Yin[1,3*]

Abstract

Background Neurovascular compression (NVC) is a primary etiology of trigeminal neuralgia (TN) and hemifacial spasm (HFS). Despite Magnetic Resonance Tomographic Angiography (MRTA) being a useful tool for 3D multimodal fusion imaging (MFI) in microvascular decompression (MVD) surgery planning, it may not visualize smaller arterial vessels and veins effectively. We validate a novel computed tomography angiography and venography (CTA/V) - diffusion tensor tractography (DTT) -3D-MFI to enhance the MVD surgical guidance.

Methods In this prospective study, 80 patients with unilateral primary TN or HFS who underwent MVD surgery were included. Imaging was conducted using CTA/V-DTT-3D-MFI compared with CT-MRTA-3D-MFI in predicting the responsible vessel and assessing the severity of NVC. Surgical outcomes were subsequently analyzed. Neurosurgery residents were provided with questionnaires to evaluate and compare the two approaches.

Results CTA/V-DTT-3D-MFI significantly improved accuracy in identifying the responsible vessel (kappa = 0.954) and NVC (kappa = 0.969) compared to CT-MRTA-3D-MFI, aligning well with surgical findings. CTA/V-DTT-3D-MFI also exhibited higher sensitivity in identifying responsible vessels (98.0%) and NVC (98.7%) than CT-MRTA-3D-MFI. Additionally, CTA/V-DTT-3D-MFI showed fewer complications, shorter operation times, and lower recurrence after one year (all $p < 0.05$). Resident neurosurgeons emphasized that CTA/V-DTT-3D-MFI greatly assisted in formulating precise surgical strategies for more accurate identification and protection of responsible vessels and nerves (all $p < 0.001$).

Conclusion CTA/V-DTT-3D-MFI enhances MVD surgery guidance, improving accuracy in identifying responsible vessels and NVC for better outcomes. This advanced imaging plays a crucial role in safer and more effective MVD surgery, as well as in training neurosurgeons.

Keywords CT arteriography and venography, Magnetic resonance tomographic angiography, Diffusion tensor tractography, Trigeminal neuralgia, Hemifacial spasm

*Correspondence:
Cheng Yin
yincheng202310@163.com
[1]The Department of Neurosurgery, Sichuan Provincial People's Hospital, University of Electronic Science and Technology of China, Chengdu 610031, China
[2]The Department of Radiology, Sichuan Provincial People's Hospital, University of Electronic Science and Technology of China, Chengdu 610031, China
[3]The Department of Neurosurgery, Sichuan Provincial People's Hospital, University of Electronic Science and Technology of China, Chengdu 610031, China

Introduction

Neurovascular compression (NVC) is a primary cause of trigeminal neuralgia (TN) and hemifacial spasm (HFS) in most cases [1]. Magnetic Resonance Tomographic Angiography (MRTA) is an effective preoperative multimodal fusion imaging (MFI) method, utilizing Magnetic Resonance Angiography (MRA) and 3D fast imaging employing steady-state acquisition (FIESTA). While MRTA provides a comprehensive understanding of NVC, it may miss small arterial vessels, arteriolar branches, and veins [2, 3].

The root entry zone (REZ) is crucial for NVC, requiring precise 3D preoperative assessment of vessel-nerve-brainstem relationships [4, 5]. Although 3D-MFI is commonly used in microvascular decompression (MVD) surgery, current research is mostly limited to 3D reconstructions from MRTA. Diffusion tensor imaging (DTI) and diffusion tensor tractography (DTT) can identify abnormalities in the cranial nerve root, which often return to normal after decompression or radiosurgery; however, there have been too few studies to establish diagnostic criteria with adequate sensitivity and specificity [6].

In this study, we introduce and evaluate a novel 3D-MFI approach to refine the limitations, which integrates computed tomography angiography and venography (CTA/V), DTT, and magnetic resonance sequences, aiming to offer a more comprehensive assessment to improve the precision of preoperative planning in MVD surgeries.

Materials and methods

Study population

This prospective study included 80 patients diagnosed with unilateral primary TN or HFS who underwent MVD surgery at the Department of Neurosurgery, Sichuan Provincial People's Hospital between January 2021 and June 2023. The inclusion criteria were as follows: (1) Classic unilateral primary TN or HFS; (2) Ineffective conservative treatment. (3) Eligible for MRI and CTA. (4) Undergo MVD surgery. The exclusion criteria were as follows: (1) TN or HFS secondary to other pathology. (2) A history of MVD surgery. (3) Contraindications for CTA or MRI.

80 patients were included, including 42 TN and 38 HFS cases. These included 35 male and 45 female patients, aged 29–75 years, with a mean [±standard deviation (SD)] age of 45.2 (±9.5) years, the disease duration was between 0.6 and 8 years, with a mean of 4.3 (±2.2) years (Table 1).

Table 1 Clinical characteristics of patients

	TN (42)	HFS (38)	ALL (80)
Sex(male/female)	17/21	18/24	35/45
Mean age(y)	47.3 ± 12.7	44.9 ± 9.6	48.3 ± 12.2
Symptomatic side(left/right)	20/22	17/21	37/43
Disease duration(y)	4.2 ± 2.5	4.5 ± 2.2	4.3 ± 2.2

Image data acquisition

Before surgery, all patients received MRTA, DTI, and CTA/V scans. The MRTA was done on a 3.0 T GE Discovery MR750 machine (USA) with 3D T1W fast spoiled gradient return sweep (FSPGR) (1 mm), 3D-FIESTA (0.4 mm), and time-of-flight (TOF)-MRA (1 mm), as well as DTI (32 directions, b = 1000 s/mm^2, 3 mm slices, no gap). CTA/V (0.625 mm slices) scans were carried out on a GE CT 750 HD machine (USA).

Image processing and analysis

A neurosurgery resident, not involved in the surgeries, and blinded to patient clinical characteristics, generated all 3D-MFI models. Digital Imaging and Communications in Medicine (DICOM) datasets were obtained and converted to Neuroimaging Informatics Technology Initiative (NIfTI) format from 3DSlicer (v4.13, http://www.slicer.org). Processing steps followed with BrainSuite (v21.a, https://brainsuite.org), 3DSlicer, and FastSurfer (v1.1.0, https://github.com/Deep-MI/FastSurfer). The pipeline included (Fig. 1):

Image Registration: 3D-T1W were used as a fixed reference. DTI were corrected for distortion and aligned using the BrainSuite Diffusion Pipeline (BDP). Additional image alignments were performed using the Advanced Normalization Tools (ANTs) in 3DSlicer.

Nerves Reconstruction: 3DSlicer's DMRI Module for DTI data import. ROIs were defined [7], and deterministic DTT traced trigeminal nerve (CN-V) and facial nerve (CN-VII/FN) fibers. Alternatively, nerves could be manually delineated using the Segment editor on registered 3D-FIESTA and 3D-T1W images [4].

Vascular Detection: Utilized 3DSlicer's Subtract Scalar Volume for CTA/V-CT analysis. Volume Rendering (VR) module identified and reconstructed vasculature from MRA and CT angiography datasets, labeling venous systems like superior petrosal vein complex (SPVC), transverse-sigmoid sinus, and mastoid emissary vein (MEV).

Brain and Skull 3D Reconstruction: Integrated 3D-T1W datasets into FastSurfer for brain segmentation, then imported into 3DSlicer for visualization. Reconstructed skull models from CT scans using VR module.

3D-MFI and Surgical Simulation: Overlaid composite models onto brainstem and cerebellum representations for 3D-MFI. Various structure reconstructions allowed options like transparency modulation. Leveraging Volume Rendering Effects, identified critical points for precise bone incisions. Analyzed skull exterior for keyhole and MEV positions, studying mastoid foramen's axial structure using CT-VR.

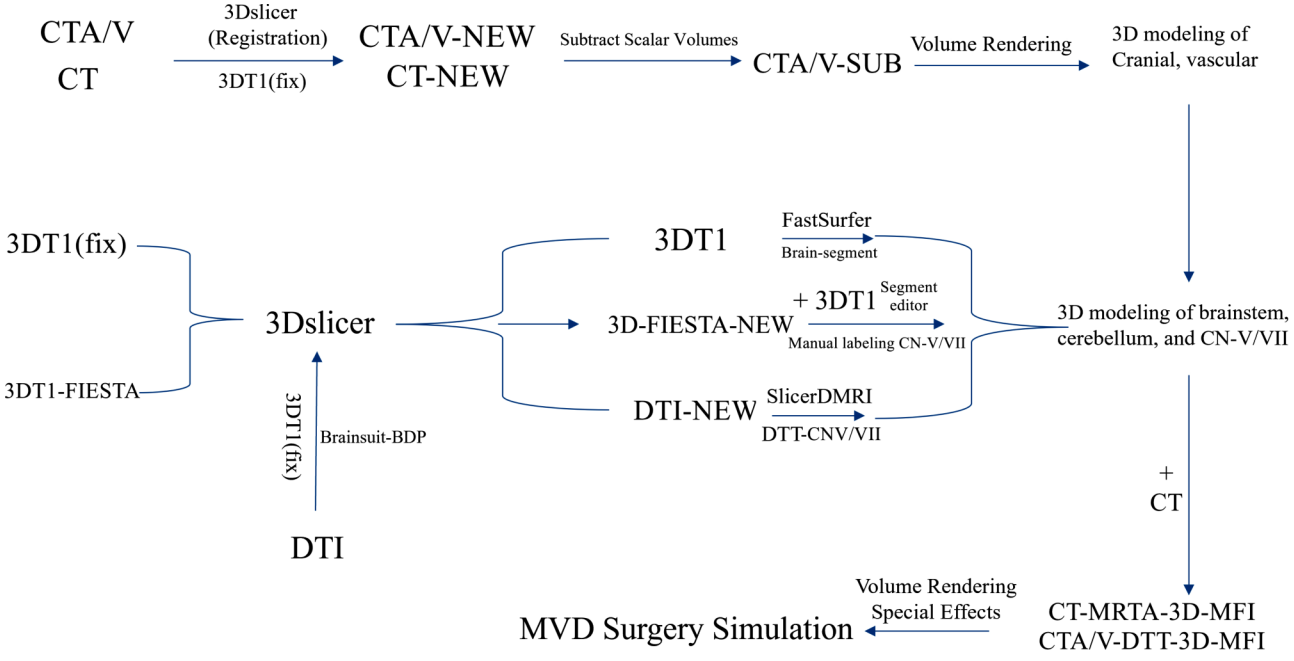

Fig. 1 Preoperative simulation process for MVD surgery

Comparative study

The patient was randomly assigned to two groups using a completely random number table. MVD surgery was performed by the same chief neurosurgeon who performed the intracerebral surgical maneuvers, assisted by the same resident who performed the craniotomy procedures. Group A: The surgeons received CT-MRTA-3D-MFI to determine the location of the mastoid foramen and keyhole, as well as nerve and vessel morphology. Group B: The surgeons received CTA/V-DTT-3D-MFI to localize the same areas and observe the morphology of the MEV and SPVC.

Responsible vessels and NVC evaluation on images

A senior neuroradiologist and a senior neurosurgeon, both blinded to the patients' clinical characteristics, collaborated to evaluate the responsible vessels and severity of NVC using CT-MRTA and CTA/V-DTT-3D-MFI models, respectively.

Surgical procedures

Consistent with the MVD surgery described by Liao et al. [4]. , but in our study, the bone flap was dissected with a milling cutter for Group A, exposing the posterior margin of the sigmoid sinus and the distal inferior margin of the transverse sinus. Group B abandoned the milling cutter when approaching the MEV and mastoid foramen, choosing a grinding drill to eliminate the remaining bone. In all cases, intraoperative electrophysiologic monitoring was employed [8, 9].

The entire procedure was videotaped, and the intraoperative view is considered the gold standard for identifying the responsible vessel and evaluating NVC.

Effect evaluation and observation index

NVC was categorized as absence (0), contact (I), compression (II), or malformation (III) [10]. Surgical efficacy [4]: complete remission (Grade I); partial remission (Grade II); ineffective (Grade III). SPV injuries refer to encompassing damage, rupture, bleeding. Observations also included surgical complications and recurrence rates at one year of follow-up.

Neurosurgical residency education

Sixteen neurosurgical residents, who have been working for one to ten years, underwent preoperative imaging and viewed the surgical video. Each resident received a questionnaire to assess the efficacy of CTA/V-DTT-3D-MFI in assisting them in comprehending surgical anatomy, determining optimal surgical views, safely isolating responsible vessels in the REZ, and formulating effective surgical plan, in comparison to CT-MRTA-3D-MFI (rated as superior, middle, or inferior).

Statistical analyses

Categorical variables compared using chi-square tests (reported as counts and percentages), and continuous variables analyzed with t-tests (presented as mean ± SD). For data categorized as ordinal, a rank-based approach, the Mann-Whitney U test, was utilized to compare groups. The kappa statistic was used to compare the

methods' accuracy in determining responsible vessel and NVC severity against surgical observations. Statistical analyses were done on SPSS 20.0, with $p<0.05$ considered significant. Kappa values for agreement were categorized as poor (<0.2), fair (0.2–0.4), moderate (0.4–0.6), good (0.6–0.8), and excellent (0.8–1.0).

Results

No significant differences in gender, age, or symptomatic side were found between groups A and B ($p>0.05$). Group B showed significant improvements over group A regarding SPV injuries, surgery time, and intraoperative hemorrhage (all $p<0.05$) (Table 2).

Group B showed improved surgical outcomes for TN compared to group A ($p=0.035$), with fewer complications for both TN ($p=0.026$) and HFS ($p=0.008$) than group A; however, there was no significant difference in HFS outcomes ($p=0.398$) between the two groups. Additionally, Group B had a lower recurrence rate after one-year follow-up (7/40,17.5%) than Group A (3/40,7.5%) (Table 2).

Group B significantly enhanced sensitivity in identifying the responsible vessel (98.0% vs. 90.0%; 78/80 vs. 72/80) with equivalent specificity (100% vs. 100%; 2/0+2 vs. 2/0+2) compared to Group A. For NVC identification, Group B demonstrated improved sensitivity (98.7% vs. 94.8%; 77/78 vs. 72/80) with equivalent specificity (100% vs. 100%; 2/0+2 vs. 2/0+2) compared to Group A. Additionally, Group B significantly improved accuracy in identifying the responsible vessel (kappa=0.954 vs. kappa=0.849) and NVC status (kappa=0.969 vs. kappa=0.821) compared to Group A, showing excellent agreement with surgical findings (Tables 3 and 4).

Neurosurgical residents' questionnaire responses indicated that the Group B were more consistent with intraoperative reality and significantly improved their understanding of surgical anatomy. This helped them to facilitate the formulation of surgical strategies that ensured identity and protection of critical vessels and nerves (all $p<0.001$) (Table 5).

Illustrative case

A patient with a four-year history of right facial pain, diagnosed with TN, was considered for MVD surgery following ineffective conservative treatment. MRTA-3D-MFI identified the right vertebral artery (VA) and posterior inferior cerebellar artery (PICA), as responsible vessels, while revealing distortion of the CN-V at REZ. However, PICA's detailed vascular anatomy could not be delineated, and the superior cerebellar arteries (SCA) were not visualized (Fig. 2A/**B**). CTA/V-DTT-3D-MFI provided enhanced visualization, showing the right

Table 2 Comparison of the craniotomy time and intraoperative hemorrhage

	Group A (CT-MRTA-3D-MFI)	Group B (CTA/V-DTT-3D-MFI)	*P* value
Sex(male/fmale)	18/22	17/23	0.822
Mean age(y)	48.1 ± 11.9	48.5 ± 12.5	0.251
Symptomatic side(L/R)	16/24	21/19	0.262
SPV injuries (case)	11/29	4/36	0.045
Surgery time (min)	95.7 ± 3.2	85.9 ± 2.1	0.000
Intraoperative hemorrhage(ml)	40.3 ± 8.2	22.5 ± 5.8	0.000
TN-Outcome			
I	12	18	-
II	7	3	-
III	2	0	0.035
TN -Complications			
Vertigo	9	5	-
Perioral herpes	7	3	-
Facial numbness	3	1	0.026
Recurrence(one-year)	4(19%)	2(9.5%)	-
HFS-Outcome			
I	14	16	-
II	4	3	-
III	1	0	0.398
HFS -Complications			
Vertigo	10	5	-
Perioral herpes	5	3	-
Facial numbness	3	0	-
Tinnitus	1	0	0.008
Recurrence(one-year)	3 (7.9%)	1 (5.3%)	-

Table 3 Comparison of responsible vessels on examination findings with intraoperative findings

	Surgical Findings							Total
		None	SCA	AICA	PICA	VA	BA	SPVC	
CT-MRTA-3D-MFI	None	3	0	0	0	0	1	3	7
	SCA	0	7	0	0	0	0	0	7
	AICA	0	0	10	3	0	0	0	13
	PICA	0	0	0	16	0	0	0	16
	VA	0	0	0	0	18	1	0	19
	BA	0	0	0	0	0	14	2	16
	SPVC	0	0	0	0	0	0	2	2
	Toal	3	7	10	19	18	16	7	80
CTA/V-DTT-3D-MFI	None	3	0	0	0	0	0	1	4
	SCA	0	7	0	0	0	0	0	7
	AICA	0	0	10	0	0	0	0	10
	PICA	0	0	0	19	0	0	0	19
	VA	0	0	0	0	18	1	0	19
	BA	0	0	0	0	0	14	1	15
	SPVC	0	0	0	0	0	0	6	6
	Toal	3	7	10	19	18	16	7	80

Table 4 Comparison of grade of NVC on examination findings with surgical findings

		Surgical Findings				Total
		0	I	II	III	
CT-MRTA-3D-MFI	0	2	4	0	0	6
	I	0	16	4	0	20
	II	0	0	36	4	40
	III	0	0	0	14	14
	Total	2	20	40	18	80
CTA/V-DTT-3D-MFI	0	2	1	0	0	3
	I	0	19	1	0	20
	II	0	0	39	0	39
	III	0	0	0	18	18
	Total	2	20	40	18	80

Table 5 Assessing the Educational Impact of CTA/V-DTT-3D-MFI and CT-MRTA-3D-MFI for neurosurgical residents

CTA/V-DTT / CT-MRTA-3D-MFI	Classification for understanding*	Consistent with intraoperative reality	How to perform more effective craniotomy	Identify vessels around nerve and REZ	Formulating rational and effective surgical plan
	Superior	16/0	16/0	16/0	16/0
	Middle	0/16	0/16	0/16	0/16
	Inferior	0/0	0/0	0/0	0/0
P value		< 0.001	< 0.001	< 0.001	< 0.001

*To determine whether CTA/V-DTT-3D-MFI is superior to CT-MRTA-3D-MFI in interpreting surgical anatomy and formulating a surgical approach

superior cerebellar artery (SCA) closely related to CN-V, and an unambiguous depiction of the entire PICA morphology. This confirmed that in its initial segment, both VA and PICA were intimately apposed and compressing the CN-V (Fig. 2C/**D**).

In the CT-VR model, the mastoid foramen is notably enlarged (2.5 mm in diameter), and a conventional craniotomy with an oblique straight incision behind the ear would inevitably lead to massive bleeding in the MEV (Fig. 3A/**C**). To circumvent this issue, we simulated a transverse incision at the bottom of the transverse sinus on the VR model, accompanied by a bone window near the mastoid foramen, thereby identifying the position for a keyhole approach (Fig. 3B/**C**). We also simulated the extent of the windowing and the operator's working field of view (Fig. 3D). During surgery, the responsible vessels were confirmed as both the VA and PICA, which was consistent with the preoperative simulations (Fig. 3E/**F**). The patient underwent successful treatment, and no recurrence was reported during the follow-up period.

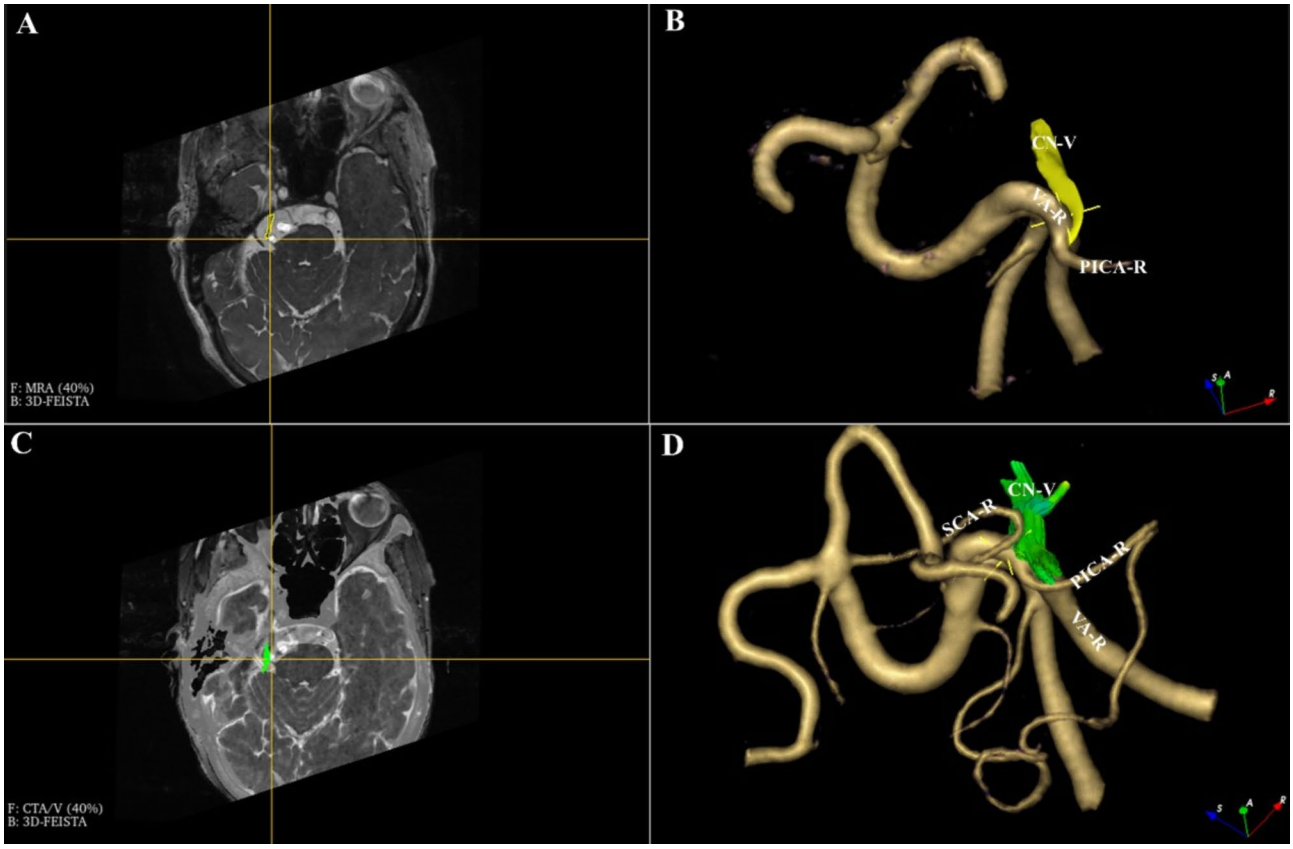

Fig. 2 Preoperative MRTA scan showing the right VA adjacent to the CN-V (yellow box) in the REZ area (yellow localized cross) (**A**). MRTA-3D-MFI model shows that the right VA and PICA are offending vessels (**B**). The preoperative CTA/V + DTT + 3DFEISTA fusion image shows the same result as compared to MRTA (**C**). The CTA/V-DTT-3D-MFI model was more detailed than the MRTA-3D-MFI model, particularly in regard to the morphology of SCA and PICA (**D**)

Discussion

TN and HFS are usually caused by NVC at the REZ, and MVD surgery is an effective treatment [1]. However, not identifying the responsible vessel before or during surgery can lead to poor outcomes. Clear preoperative 3D imaging of the skull, nerves, and vessels is essential for safe and effective MVD surgery [4].

MRTA is conducted to identify the responsible vessel and NVC in the REZ with a high degree of consistency compared to intraoperative vascular compression of nerves [11]. MRTA-3D-MFI further provides surgeons with more accurate determination of the responsible vessel and NVC than MRTA [4, 5, 12, 13]. However, MRTA may have limited visibility in slow-flowing veins and small arteries, which can hinder a comprehensive assessment of the responsible vessel, potentially leading to missed or misdiagnoses [14].

CTA/V is widely used for diagnosing cerebrovascular diseases and aligns well with digital subtraction angiography (DSA), the gold standard [15]. Gospodarev et al. [16]. used CTA and CT cisternography with MFI in a TN patient who couldn't undergo MRI, successfully mimicking MRTA, identifying the vessel, and executing the procedure. Iwata et al. [17]. compared CTA-3D-MFI and MRTA-3D-MFI to improve MVD surgical simulation accuracy in HFS and TN patients, though only in four cases. Both studies suggest CTA may be an alternative for identifying the offending vessel in MVD surgery.

MVD surgery is performed through the retrosigmoid approach. However, errors in locating the keyhole (IMTS) using the star point as a marker have been noted [4]. Neuro-navigation ensures precise localization, but not all neurosurgical departments, especially in developing countries, can afford such systems. Liao et al. [4]. showed that 3D preoperative planning with CT-MRTA-3D-MFI via 3DSlicer can assist MVD surgery, but they overlooked the importance of the mastoid foramen, MEV, and SPVC. Recognizing the mastoid foramen and MEV is crucial, especially in elderly patients with significant dural adhesion, as injury to these structures can cause significant bleeding and other serious complications [18].

The SPVC is the main obstacle in the retrosigmoid approach. As the responsible vessel, it often adheres to and compresses the CN-V, sometimes even crossing the nerve. Proper management of the SPVC during MVD surgery is debated, as preserving it minimizes

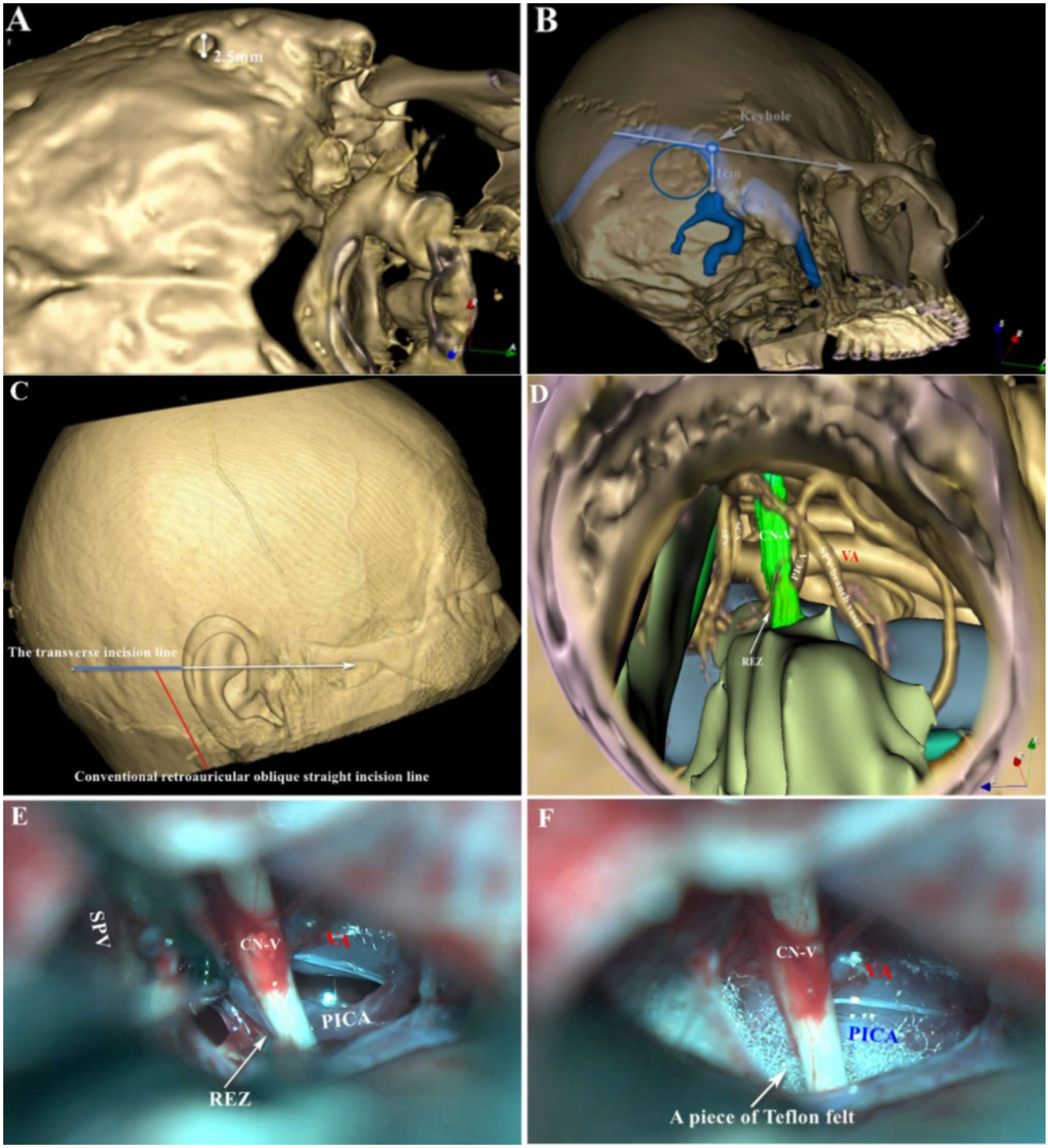

Fig. 3 CT-VR reconstruction reveals an enlarged mastoid foramen (2.5 mm in diameter) (**A**). Keyhole positioning is flush with the zygomatic arch's inferior margin, orthogonal to the line extending from the digastric groove's point (1 cm distally). Simulated extent of bone window removal illustrated by the blue coil (**B**). Simulations depict a transverse incision at the transverse sinus's base and a retroauricular oblique incision, with the former selected (**C**). Unobstructed visualization of CN-V, neighboring SPVC, and positions of PICA, VA, and SCA in the simulation (**D**). Intraoperative examination confirms spatial relationship between CN-V, REZ, SPV, PICA, and VA, corroborating preoperative simulations (**E**). Teflon felt strategically placed intraoperatively to segregate CN-V from PICA and VA (**F**)

complications like cerebellar/brainstem edema, infarction, hemorrhage, or death [19, 20]. Therefore, a comprehensive understanding of SPVC anatomy through preoperative imaging is crucial. Tanriover et al. [21]. suggest that preoperative MRV or CTV can reveal the SPVC on 3D imaging, aiding in planning retrosigmoid approaches and reducing venous complications.

Identifying nerve deformities on 2D MRTA is difficult due to inadequate contrast with CSF, which can lead to inaccuracies in depicting nerve shape [2]. Oishi et al. [22]. employed interactive 3D virtual simulation using 3D-CISS, TOF-MRA, and CTA/V data in MVD surgeries, improving preoperative visualization of neurovascular structures in patients with trigeminal neuralgia and hemifacial spasm. This method achieved a 96% accuracy rate in pinpointing compression causes, outperforming conventional 2D imaging, which had a 73% accuracy. However, manual annotation of cranial nerves in routine MRI sequences, especially CN-V and FN near the brainstem, is difficult due to similar signal intensities. This similarity complicates automatic differentiation and accurate annotation on both 2D and 3D images, exacerbated when nerves are compressed by nearby blood vessels, further hindering REZ identification.

DTI measures water molecule diffusion in the brain's white matter and cranial nerves. It often encounters challenges with magnetic field irregularities (B0) in echo planar imaging (EPI) sequences, especially around air and the skull base bone, causing localized distortions, particularly in areas like the skull base and frontal regions [23]. BDP corrects these distortions effectively using 3D-T1W images as a reference [24]. DTT, derived from DTI, reconstructs white matter tracts and cranial nerves in 3D [7, 25]. Sano et al. [26]. utilized the MRTA-DTT-3D-MFI model to precisely assess the REZ of the facial nerve (FN) and its associated vasculature before and after microvascular decompression (MVD) surgery for hemifacial spasm (HFS), facilitating detailed surgical planning based on their intricate relationship. Haller et al.'s review demonstrated tractography reconstruction revealing a slightly reduced fiber count on the right side compared to the left in a patient with right-sided trigeminal neuralgia (TN) [27].

To improve preoperative procedures, we replaced TOF-MRA with CTA/V and integrated multimodal fusion of 3D-T1W, 3D-FIESTA, and DTI sequences. This approach aims to improve identification of the responsible vessel, assess severity of NVC, enhance accuracy in locating the mastoid foramen, MEV, and SPVC, and facilitate surgical planning. Our surgical findings indicate that the CTA/V-DTT-3D-MFI approach demonstrated superior sensitivity (98.0% vs. 90.0%) and excellent agreement in identifying the responsible vessel (Kappa=0.954), outperforming the CT-MRTA-3D-MFI approach (Kappa=0.849). CTA/V provides detailed vascular anatomy insights, aiding in surgical approach determination and prognosis prediction for trigeminal neuralgia (TN) and hemifacial spasm (HFS) caused by venous compression [28]. It also helps rule out vascular diseases in the cerebellopontine angle (CPA), reducing unnecessary surgical exploration and minimizing risks of nerve and vessel injuries, thereby lowering surgical complications [29, 30]. For instance, if CTA indicates a close connection between the superior petrosal vein complex (SPVC) and the trigeminal nerve (CN-V) in TN patients, surgeons may consider performing a partial sensory trigeminal rhizotomy (PSR) to enhance surgical outcomes [31].

In addition, The CTA/V-DTT-3D-MFI group showed significant improvements in outcomes compared to the CT-MRTA-3D-MFI group. These included reduced SPV injury, shorter operative time, less intraoperative bleeding, fewer complications, and a lower one-year recurrence rate. The enhanced postoperative effectiveness of the CTA/V-DTT-3D-MFI group is attributed to detailed preoperative assessment of relevant arteries and veins, facilitating better planning and intraoperative management. Importantly, there was no difference in postoperative outcomes in HFS, likely because MRTA effectively identifies the predominantly arterial responsible vessels in most cases, as noted by Busse et al. [32].

Prior studies have established a correlation between the severity of NVC and the efficacy of TN and HFS-MVD surgical interventions [33, 34]. Leal et al. [35]. suggested that MVD represents the preferred therapeutic approach for NVC of Grade II or III. Yet, for elderly patients with vulnerable health conditions and NVC of Grade I, alternative interventions such as percutaneous lesioning procedure or radiosurgery might be more appropriate. Hao et al. [11]. found a strong agreement (Kappa=0.770) between preoperative MRTA and intraoperative assessments in NVC determination during MVD surgery. Our study revealed that the CTA/V-DTT-3D-MFI group exhibited enhanced sensitivity (98.7% vs. 94.8%) and excellent agreement in NVC assessment (Kappa=0.969), surpassing the CT-MRTA-3D-MFI group (Kappa=0.821) based on surgical findings.

Highly detailed imaging may not be indispensable for experienced MVD surgeons who rely on intraoperative exploration. However, gaining such proficiency requires considerable time and experience, which cannot achieve quickly. Therefore, advanced CTA/V-DTT-3D-MFI imaging is crucial for aiding in the planning and refinement of MVD surgical procedures for inexperienced surgeon. It also plays a significant role in the training of neurosurgeons, as affirmed by their questionnaire responses.

By involving residents in evaluating imaging modalities, we aimed to capture the perspective of

surgeons-in-training, who are crucially developing their skills in surgical planning and execution. These individuals are highly receptive to advancements in technology that could enhance their learning curve and future performance. Their feedback offers valuable insights into how emerging technologies like CTA/V-DTT-3D-MFI can support the education of future neurosurgeons, ensuring they integrate sophisticated imaging early in their careers. Additionally, using surgical videos as a benchmark provides a practical reference to validate the accuracy and utility of the imaging techniques studied. This approach strengthens our findings by directly comparing imaging-guided predictions with surgical outcomes, confirming the superiority of CTA/V-DTT-3D-MFI in identifying responsible vessels, assessing NVC, and guiding overall surgical procedures.

In all, CTA/V-DTT-3D-MFI exhibits better specificity in predicting the responsible vessel and NVC, nearly perfect representation of real surgical anatomy, and enables more accurate preoperative MVD surgical simulations. In addition, DTI allows quantitative measurement and analysis of the microstructure of nerve fibers and predicts the prognosis of TN and HFS patients during follow-up [36, 37].

Limitations

The study has several methodological limitations. The small sample size may not provide sufficient statistical power for broad generalization. Conducting the study at a single center restricts external validity, necessitating multicenter trials. Involving neurosurgery residents with varying experience levels introduces potential variability, affecting reliability. The one-year follow-up period may not adequately evaluate long-term outcomes. CTA is not recommended for patients with contraindications to contrast or radiation, limiting its practical applicability.

Conclusion

CTA/V-DTT-3D-MFI enhances MVD surgery guidance, improving accuracy in identifying responsible vessels and NVC for better outcomes. This advanced imaging plays a crucial role in safer and more effective MVD surgery, as well as in training neurosurgeons.

Author contributions

All authors made an intellectual contribution through discussion at a consensus meeting and approved the manuscript. Paper writing: Xiaolin Hou. Paper reviewing: Cheng Yin. Study supervision: Ru xiang Xu, Jing Tang. Intellectual content: all authors.

Funding

This work was funded by grants from the National Natural Science Foundation of China (No. 82071318, 2020).

Data availability

The datasets used and/or analyzed during the current study are available from the corresponding author on reasonable request.

Declarations

Ethical approval

The study received ethical approval from the Ethics Committee of Sichuan Provincial People's Hospital (No. 82071318, 2020).

Consent for publication

The present study was conducted in accordance with the tenets of the 1975 Declaration of Helsinki. All participants provided written informed consent before investigations, screening, study and treatment. Written informed consent for publication of the participant images and clinical details were obtained from each patient.

Competing interests

The authors declare no competing interests.

Received: 19 February 2024 / Accepted: 31 July 2024
Published online: 10 October 2024

References

1. Min L, Liu M, Zhang W, Tao B, Sun Q, Li S, et al. Outcomes and safety of overlapping surgery in patients undergoing microvascular decompression for Hemifacial Spasm and Trigeminal Neuralgia. World Neurosurg. 2019;130:e1084–10841090.
2. Fukuda H, Ishikawa M, Okumura R. Demonstration of neurovascular compression in trigeminal neuralgia and hemifacial spasm with magnetic resonance imaging: comparison with surgical findings in 60 consecutive cases. Surg Neurol. 2003;59(2):93–9. discussion 99–100.
3. Zhang W, Chen M, Zhang W, Chai Y. Etiologic exploration of magnetic resonance tomographic angiography negative trigeminal neuralgia. J Clin Neurosci. 2014;21(8):1349–54.
4. Liao CC, Wu KH, Chen G. Application of Preoperative Multimodal Image Fusion technique in microvascular decompression surgery via Suboccipital Retrosigmoid Approach. World Neurosurg. 2023;173:e37–3747.
5. Teton ZE, Blatt D, Holste K, Raslan AM, Burchiel KJ. Utilization of 3D imaging reconstructions and assessment of symptom-free survival after microvascular decompression of the facial nerve in hemifacial spasm. J Neurosurg. 2019:1–8.
6. Cruccu G, Finnerup NB, Jensen TS, Scholz J, Sindou M, Svensson P, et al. Trigeminal neuralgia: new classification and diagnostic grading for practice and research. Neurology. 2016;87(2):220–8.
7. Yoshino M, Abhinav K, Yeh FC, Panesar S, Fernandes D, Pathak S, et al. Visualization of cranial nerves using high-definition Fiber Tractography. Neurosurgery. 2016;79(1):146–65.
8. Thirumala PD, Altibi AM, Chang R, Saca EE, Iyengar P, Reddy R, et al. The utility of intraoperative lateral spread Recording in Microvascular Decompression for Hemifacial Spasm: a systematic review and Meta-analysis. Neurosurgery. 2020;87(4):E473–473484.
9. Zhao YX, Miao SH, Tang YZ, He LL, Yang LQ, Ma Y, et al. Trigeminal somatosensory-evoked potential: a neurophysiological tool to monitor the extent of lesion of ganglion radiofrequency thermocoagulation in idiopathic trigeminal neuralgia: a case-control study. Med (Baltim). 2017;96(3):e5872.
10. Jani RH, Hughes MA, Gold MS, Branstetter BF, Ligus ZE, Sekula RF Jr. Trigeminal nerve Compression without Trigeminal Neuralgia: intraoperative vs imaging evidence. Neurosurgery. 2019;84(1):60–5.
11. Hao YB, Zhang WJ, Chen MJ, Chai Y, Zhang WH, Wei WB. Sensitivity of magnetic resonance tomographic angiography for detecting the degree of neurovascular compression in trigeminal neuralgia. Neurol Sci. 2020;41(10):2947–51.
12. Han KW, Zhang DF, Chen JG, Hou LJ. Presurgical visualization of the neurovascular relationship in trigeminal neuralgia with 3D modeling using free slicer software. Acta Neurochir (Wien). 2016;158(11):2195–201.
13. Yao S, Zhang J, Zhao Y, Hou Y, Xu X, Zhang Z, et al. Multimodal Image-based virtual reality Presurgical Simulation and evaluation for trigeminal Neuralgia and Hemifacial Spasm. World Neurosurg. 2018;113:e499–499507.
14. Han-Bing S, Wei-Guo Z, Jun Z, Ning L, Jian-Kang S, Yu C. Predicting the outcome of microvascular decompression for trigeminal neuralgia using magnetic resonance tomographic angiography. J Neuroimaging. 2010;20(4):345–9.

15. Gemmete JJ, Chaudhary N, Pandey AS, Oweis Y, Thompson BG, Maher CO, et al. Initial experience with a combined multidetector CT and biplane digital subtraction angiography suite with a single interactive table for the diagnosis and treatment of neurovascular disease. J Neurointerv Surg. 2013;5(1):73–80.
16. Gospodarev V, Chakravarthy V, Harms C, Myers H, Kaplan B, Kim E, et al. Computed tomography cisternography for evaluation of trigeminal Neuralgia when magnetic resonance imaging is contraindicated: Case Report and Review of the literature. World Neurosurg. 2018;113:180–3.
17. Iwata T, Hosomi K, Tani N, Khoo HM, Oshino S, Kishima H. Utilization of three-dimensional fusion images with high-resolution computed tomography angiography for preoperative evaluation of microvascular decompression: patient series. J Neurosurg Case Lessons. 2023;6(9):CASE23330.
18. Hampl M, Kachlik D, Kikalova K, Riemer R, Halaj M, Novak V, et al. Mastoid foramen, mastoid emissary vein and clinical implications in neurosurgery. Acta Neurochir (Wien). 2018;160(7):1473–82.
19. Kasuya H, Tani S, Kubota Y, Yokosako S, Ohbuchi H, Arai N, et al. Characteristics and management of the offending veins in microvascular decompression surgery for trigeminal neuralgia. Neurosurg Rev. 2021;44(4):2337–47.
20. Liebelt BD, Barber SM, Desai VR, Harper R, Zhang J, Parrish R, et al. Superior Petrosal Vein Sacrifice during Microvascular Decompression: Perioperative Complication Rates and comparison with venous preservation. World Neurosurg. 2017;104:788–94.
21. Tanriover N, Abe H, Rhoton AL Jr, Kawashima M, Sanus GZ, Akar Z. Microsurgical anatomy of the superior petrosal venous complex: new classifications and implications for subtemporal transtentorial and retrosigmoid suprameatal approaches. J Neurosurg. 2007;106(6):1041–50.
22. Oishi M, Fukuda M, Hiraishi T, Yajima N, Sato Y, Fujii Y. Interactive virtual simulation using a 3D computer graphics model for microvascular decompression surgery. J Neurosurg. 2012;117(3):555–65.
23. Techavipoo U, Okai AF, Lackey J, Shi J, Dresner MA, Leist TP, et al. Toward a practical protocol for human optic nerve DTI with EPI geometric distortion correction. J Magn Reson Imaging. 2009;30(4):699–707.
24. Bhushan C, Haldar JP, Choi S, Joshi AA, Shattuck DW, Leahy RM. Co-registration and distortion correction of diffusion and anatomical images based on inverse contrast normalization. NeuroImage. 2015;115:269–80.
25. Xie G, Zhang F, Leung L, Mooney MA, Epprecht L, Norton I, et al. Anatomical assessment of trigeminal nerve tractography using diffusion MRI: a comparison of acquisition b-values and single- and multi-fiber tracking strategies. Neuroimage Clin. 2020;25:102160.
26. Sano K, Kuge A, Kondo R, Yamaki T, Nakamura K, Saito S, et al. Ingenuity using 3D-MRI fusion image in evaluation before and after microvascular decompression for hemifacial spasm. Surg Neurol Int. 2022;13:209.
27. Haller S, Etienne L, Kövari E, Varoquaux AD, Urbach H, Becker M. Imaging of Neurovascular Compression syndromes: trigeminal neuralgia, Hemifacial Spasm, vestibular paroxysmia, and Glossopharyngeal Neuralgia. AJNR Am J Neuroradiol. 2016;37(8):1384–92.
28. Toda H, Iwasaki K, Yoshimoto N, Miki Y, Hashikata H, Goto M, et al. Bridging veins and veins of the brainstem in microvascular decompression surgery for trigeminal neuralgia and hemifacial spasm. Neurosurg Focus. 2018;45(1):E2.
29. Dou NN, Hua XM, Zhong J, Li ST. A successful treatment of coexistent hemifacial spasm and trigeminal neuralgia caused by a huge cerebral arteriovenous malformation: a case report. J Craniofac Surg. 2014;25(3):907–10.
30. Komatsu F, Sasaki K, Tanaka R, Miyatani K, Yamada Y, Kato Y, et al. Coexistence of neurovascular compression syndrome and unruptured cerebral aneurysm. J Clin Neurosci. 2022;105:22–5.
31. Liu R, Deng Z, Zhang L, Liu Y, Wang Z, Yu Y. The long-term outcomes and predictors of microvascular decompression with or without partial sensory rhizotomy for trigeminal Neuralgia. J Pain Res. 2020;13:301–12.
32. Busse S, Taylor J, Field M. Correlation of Preoperative High-Resolution Neurovascular Imaging and Surgical Success in Neurovascular Compression syndromes. World Neurosurg. 2023;172:e593–593598.
33. Hughes MA, Jani RH, Fakhran S, Chang YF, Branstetter BF, Thirumala PD et al. Significance of degree of neurovascular compression in surgery for trigeminal neuralgia. J Neurosurg. 2019:1–6.
34. Zhang P, Selim MH, Wang H, Kuang W, Wu M, Ji C, et al. Intraoperative measuring of the Offending Vessel's pressure on the facial nerve at Root Exit Zone in patients with Hemifacial Spasm during Microvascular Decompression: a prospective study. World Neurosurg. 2019;122:e89–8995.
35. Leal PR, Hermier M, Souza MA, Cristino-Filho G, Froment JC, Sindou M. Visualization of vascular compression of the trigeminal nerve with high-resolution 3T MRI: a prospective study comparing preoperative imaging analysis to surgical findings in 40 consecutive patients who underwent microvascular decompression for trigeminal neuralgia. Neurosurgery. 2011;69(1):15–25. discussion 26.
36. Jin Z, Li Z. Clinical application of Diffusion Tensor Imaging in diagnosis and prognosis of Hemifacial Spasm. World Neurosurg. 2021;145:e14–1420.
37. Lutz J, Thon N, Stahl R, Lummel N, Tonn JC, Linn J, et al. Microstructural alterations in trigeminal neuralgia determined by diffusion tensor imaging are independent of symptom duration, severity, and type of neurovascular conflict. J Neurosurg. 2016;124(3):823–30.

Publisher's Note